Solvation of the Hydroxide Anion: A Combined DFT and Molecular Dynamics Study

Dongqing Wei,*,‡ E. I. Proynov,†,§ A. Milet,† and D. R. Salahub‡,†,||

Département de chimie, Université de Montréal, C.P. 6128 Succursale Centre-ville, Montréal, Québec, H3C 3J7, Canada, and Centre de Recherche en Calcul Appliqué (CERCA), 5160, boul. Décarie, bureau 400, Montreal, Quebec, H3X 2H9 Canada, and Laboratoire de Chimie Théorique Appliquée, Facultés Universitaires Notre Dame de la Paix, 61 rue de Bruxelles, 5000 Namur, Belgium

Received: July 22, 1999; In Final Form: November 30, 1999

The electronic structure of solvated hydroxide complexes $((OH)^- H_2O)_n$, $n = 1-3$, is studied in detail using density functional theory (DFT), MP2, and Born−Oppenheimer-Molecular Dynamics (BOMD) approaches. Several nonlocal functionals of the GGA and LAP families are employed, special attention is paid to the reliability of the LAP functionals in predicting structure, energetics, and proton transfer barriers. It is found that most of these give reasonable energetics of the quite strong hydrogen bonding in hydroxide anions (within a difference of about 2−15% from the experimental solvation enthalpies), provided that basis sets with both polarization and diffuse functions are employed and the basis set superposition error is taken care of. The performance of the various methods for the geometry of the hydroxide complexes is not so uniform, especially for the hydrogen bond distances and the shape of the complex with three water ligands. These differences are reflected also in the calculated vibrational spectra, particularly concerning the vibrations involving the hydrogen bonds. For $O_2H_3^-$, the potential energy surface associated with the central proton degrees of freedom is very flat, which leads to an intriguing proton dynamics. The BOMD simulation shows that the proton population profile is rather similar for BP and PP functionals, while the dynamical proton-transfer counting autocorrelation function, is, on the other hand, very sensitive to the choice of functional.

1. Introduction

The correct description of hydrogen bonds is very important in theoretical modeling of biochemical systems. Recent high quality calculations have demonstrated the significance of electron correlation in the subtle energetics and dynamics of hydrogen bonds.[1−3] In this vein, density functional theory (DFT) has become a promising alternative to the computationally more demanding post-Hartree−Fock (HF) methods. The development of nonlocal exchange-correlation schemes of the generalized gradient approximation (GGA) type over the past decade or so[4−6] has led to substantial progress in the DFT description of hydrogen-bond structure and energetics.[1,7] However, further improvement is still needed, especially concerning hydrogen bond distances (somewhat shortened by the GGA) and intramolecular proton-transfer barriers (quite underestimated by the GGA).[8] The recent hybrid HF-DFT schemes[9,10] offer a substantial improvement for many covalently bonded systems, whereas for weak hydrogen bonds typical results show a moderate improvement over the GGA.[1,8,11,12]

Another type of functional giving an improved description of hydrogen bonded systems has been recently constructed by combining the GGA exchange functionals of Becke[4] and Perdew[5] with the kinetic-energy-density (τ) and Laplacian-dependent correlation functionals LAP1 and LAP3.[12,13] The resulting XC schemes BLAP1, BLAP3 (GGA exchange of Becke[4] plus LAP1(LAP3) correlation[12,13]) and PLAP1, PLAP3 (GGA exchange of Perdew[5] plus LAP correlation) yielded improved hydrogen bond distances, often very close to the experimental estimates.[1,8,12,13] They also provided a correct DFT description of the subtle electronic structure of the lowest glycine conformers, and gave results very close to the G2 composite estimate for the intramolecular proton-transfer barrier in malonaldehyde[8] and the barrier of hydrogen abstraction.[14] These, as well as various other DFT studies,[1,2,15] have provided a certain validation of various DFT techniques for weak neutral hydrogen-bonded systems.

Relatively fewer studies have been reported so far on hydrogen bonding in charged systems. Positively charged systems of the type $(H_3O^+)(H_2O)_n$ have been thoroughly studied recently by a combined Kohn−Sham (KS) DFT-Born−Oppenheimer molecular dynamics (BOMD) algorithm in ref 16. Negatively charged hydrogen-bonded systems are anticipated to be more difficult, due to some intrinsic problems that approximate XC functionals still meet. Hydrogen bonds involving negatively charged groups are very important ingredients of biological systems. The significant role of the cooperative hydrogen bond interactions in such systems has been reviewed and studied in detail in ref 1. Studying such systems is also very important for atmospheric physics[17] and for understanding in more detail proton-transfer processes in chemistry and biochemistry,[16] particularly in enzyme catalysis.[18,19] Some anionic H-bonded systems (including $(OH)^- H_2O$) were studied recently by Pudzianowski[20,21] using the BLYP functional (GGA exchange of Becke[4] plus Lee−Yang−Parr correlation[6]) and its hybrid HF-DFT extension B3LYP.[6,9,10] It was pointed out that the choice of basis set is very important in DFT treatments of anionic systems, and the inclusion of diffuse and polarization functions is mandatory.

A very recent quantum dynamical study of $H_5O_2^+$ and $H_3O_2^-$ has been reported in ref 22 based on Feynman's path integral and Car−Parrinello type techniques.

† Département de Chimie.
‡ CERCA.
§ Laboratoire de Chimie Théorique Appliqué.
|| Present address: Steacie Institute for Molecular Sciences, National Research Council of Canada, 100 Sussex Drive, Ottawa, K1A 0R6 Ontario.

10.1021/jp992540s CCC: $19.00
Published on Web 02/16/2000

We present a detailed study of solvated hydroxide anion complexes $(OH\text{-})(H_2O)_n$, applying, for the first time, the Lap functionals to negatively charged systems in conjunction with BOMD simulations to study the proton-transfer dynamics. For $O_2H_3^-$, all methods show a strong H-bond formation between OH^- and H_2O, with a low proton transfer barrier. GGA gives this barrier too low. Overall, the results, especially for geometries, are quite sensitive to the method used. This makes it important to compare results from several different methods, keeping the numerical precision at the maximum available level, to gain an objective quantitative knowledge about these subtle systems. Another objective of the present study is to compare the behavior of solvated anions, such as $H_3O_2^-$, with that of the solvated hydronium H_3O^+ ion studied in detail previously.[16]

Turning first to the experimental side, while for systems such as $(H_2O)_n$ and $(H_3O^+)(H_2O)_n$ more detailed structural, vibrational, and thermodynamic data are available in the literature, for $(OH^-)(H_2O)_n$ only the enthalpies and entropies of hydration for the consecutive association of a few water molecules have been reported so far. In the experimental study of Mautner[23] the enthalpies of successive association of water molecules (from $n = 1$ to $n = 7$) to OH^- were determined by a pulsed high-pressure mass spectrometer method as -26.5, -17.6, -16.2, -12.0, -11.5, -11.2, and -10.3 kcal/mol, respectively, indicating a solvation shell effect, i.e., after $n = 3$, the water molecules start to fill the second solvation shell. This also means that OH^- does not have a four coordinated solvation structure in small hydration clusters. These experimental values (with a reported error bar about ± 1.0 kcal/mol) are in good agreement with the estimates of Kebarle et al.[24] (-25.0 kcal/mol for $n = 1$ and -17.9 kcal/mol for $n = 2$) using a pulsed method similar to that of ref 23. The latter study revised the values of 22.0 kcal/mol (for $n = 1$) and 16.0 kcal/mol (for $n = 2$) found previously by the same authors with a continuous ionization method.[25] The good agreement between the results of ref 23 and ref 24 lends confidence to the experimental enthalpies reported by these authors, while the earlier estimate -34.0 kcal/mol (for $n = 1$) by De Paz et al.[26] seems to be overestimated.

On the theoretical side, various high quality ab initio calculations have been devoted to these aqua complex anions.[20,22,32,33,35] It is worth emphasizing once more that the use of basis sets with diffuse functions and methods incorporating electron correlation has been found essential, required by the anionic character of these systems and the specific nature of the hydrogen bonds there.

The early studies along these lines were confined mainly to the case of one solvent water $H_3O_2^-$.[27−29] The Hartree−Fock approximation fails to reproduce well the experimental data, whatever basis sets are used.[27,30,31] The lack of diffuse functions in the basis set used in the earlier MP2 calculations[27−29] resulted in an almost symmetric O···H···O bridge between the OH^- ion and the water molecule, and the MP2 solvation energy was too large compared to the experimental estimate.

Several more recent studies reported fully optimized results for $(OH^-)(H_2O)_n$ using correlated ab initio methods with larger basis sets.[20,21,32,33] Xantheas[32] considered the cases of $n = 1,2$, and 3, using a flexible aug-cc-VDZ basis set[34] at the MP2 level. The MP2 results with this basis set were within the experimental error bars, except for $n = 2$, where the MP2 solvation energy was somewhat larger. Grimm et al.[33] optimized the same systems using a smaller basis set with polarization and diffuse functions DZP(s,p), again at the MP2 level (for $n = 1-4$) and at the HF level for $n = 5$. It was reconfirmed that the HF approximation is not suitable for such systems. Due to these and other high quality theoretical studies[22] the geometry of $H_3O_2^-$ has been established as asymmetric, with a longer O···H distance of about 1.4 Å and a shorter distance of about 1.09 Å.[32] The geometry features of $H_3O_2^-$ are thus somewhat different from those of the solvated hydronium H_3O^+ ion,[16] where the H-bond is symmetric. This is perhaps because the positive charge is located in a symmetric way there (in the middle of the bridge), while in the case of $O_2H_3^-$ the negative charge is localized predominantly on one side of the bridge. It should be noted that the precise optimization of the H-bond geometry in these systems is a very demanding task because the energy barrier for proton transfer is very low[16,32] and the energy minimum with respect to these degrees of freedom is very flat,[16] facts that we will return to later on in the discussions.

Based on Feynman's path integral and Car−Parrinello type techniques it was shown in ref 22 that the shared proton in $H_5O_2^+$ has a predominantly classical behavior, while the shared proton in the $H_3O_2^-$ anion has a noticeable quantum character influencing the nature of the low-barrier hydrogen bonding. When the proton is treated as classical, the hydrogen bond in $H_3O_2^-$ was indeed found to be asymmetric, associated with a double well of the hydrogen-bond effective potential. However, the quantum motion of the proton smears out the double-peak structure of the effective potential.[22] Our results will show that the predicted position of the proton depends sensitively on the method and the basis set used in the calculation.

Concerning calculations of the enthalpies of successive association, the MP4/6-31+G(2p,2d) estimates[35] and the MP2/aug-cc-VDZ estimates[32] reproduce well and support the experimental data of Mautner[23] and Kebarle.[24] Among the best DFT results available for the enthalpy of association of $H_3O_2^-$ ($n = 1$), are the recent calculations by Pudzianowski[20] using hybrid (B3LYP) and GGA (BLYP) functionals. Both functionals tend to overestimate the binding energy compared to the experimental data and MP2: the best DFT value reported in ref 20 is -29.4 kcal/mol obtained at the B3LYP/6311++G(d,p) level, about 4 kcal/mol too high. BLYP gives a similar (but slightly worse) energy estimate, compared to B3LYP with the same basis set.[20,22]

In the present work, the equilibrium geometries, binding energies and vibrational analysis of $(OH^-)(H_2O)_n$ (for n up to 3) are calculated using several nonlocal XC functionals. The performance of the τ-dependent XC schemes BLAP3 and PLAP3 [12] is of particular interest to us, since these functionals are examined here for the first time on this type of H-bonds. The GGA schemes of Becke exchange−Perdew correlation (BP) and Perdew exchange−Perdew correlation[5] (PP) are also used for comparison, and for some of the systems the hybrid HF-DFT scheme B3LYP is employed. The influence of the basis set is also examined in detail. The BOMD simulation reveals some striking difference between a "dynamical" and optimized structure for $n = 1$ at 0 K, showing that the proton position has to be viewed (within classical mechanics) as a dynamical variable, since the thermal fluctuations at 300 K can easily overcome the low proton-transfer barrier in this system. We calculated the proton-transfer counting correlation function, which provided a direct means to study the proton dynamics. The result shows that, unlike the proton profile, the dynamics is very sensitive to the level of theory used.

2. Computational Details

The KS-DFT calculations with the GGA functionals BP and PP, and the τ -dependent schemes BLAP3, PLAP3[12] were carried out using the latest version of the LCGTO-DFT program

deMon-KS3.[36,37] We have tested several orbital basis sets with different size to address the issue of the basis set sensitivity. Satisfactory results were obtained when the bases include diffuse functions, in agreement with other studies of similar systems. Three suitable basis sets were selected: two having split valence plus polarization and diffuse functions of the type 631++G(*,*) and 6311++G(*,*) basis,[38] and the more flexible pVTZ basis of Sadlej,[39] designed to reproduce computationally demanding electronic properties. Although these basis sets were not particularly optimized for deMon-KS3 DFT calculations within a chosen functional (which should be the optimal way of proceeding[40]), various tests have validated their suitability in the present calculations.

Auxiliary charge density (CD) and exchange-correlation (XC) fitting basis sets consisting of four s functions and four sets of s, p, and d functions with common exponents were used for oxygen (denoted as (4,4;4,4)) while (5,1;5,1) auxiliary patterns were used for all H atoms. We have verified the quality of these fitting bases in several ways, including comparisons with results obtained with Gaussian94[41] (where fitting is not employed) using identical functional (BP) and basis set.

The geometries were optimized until both the norm of the total energy gradient (averaged over the atoms) and the norm of the maximal individual gradient, fell below a threshold of 0.0001 au, using the Broyden−Fletcher−Goldfarb−Shanno (BFGS) algorithm.[42] Concerning the geometry optimization with the LAP schemes, it should be noted that these are not fully self-consistent with respect to the correlation potential: the nonlocal corrections enter only the correlation energy expression while in the corresponding correlation potential these corrections are omitted.[12] Despite this, geometry optimizations with the LAP3 schemes have proven to be very efficient, often giving results better than the GGA geometry estimates, especially for weak H-bond lengths,[12,8] which is mainly due to the correct long-range asymptotics this correlation potential possesses.

To compare our results with the experimental data, the binding energies have been corrected for the basis set superposition error (bsse) by the counterpoise (CP) method of Boys and Bernardi.[43] For a reaction of the type:

$$\mathbf{A} + \mathbf{B} \rightarrow \mathbf{AB}$$

where **A** stands for OH^- and **B** for H_2O, the binding energy is calculated as

$$\Delta E_b = E_{\mathbf{AB}}^{\alpha\cup\beta}(\mathbf{AB}) - [E_{\mathbf{A}}^{\alpha}(\mathbf{A}) + E_{\mathbf{B}}^{\beta}(\mathbf{B})] \quad (1)$$

The molecule, whose energy is computed, is indicated in parentheses. The superscripts denote the basis set used: the basis of A is denoted as α and that of **B**, β. Consequently, the basis set of **AB** is denoted as $\alpha\cup\beta$. The subscripts indicate the optimized structure used in the calculation. With this notation, the bsse correction is calculated as

$$\delta E_{CP} = E_{\mathbf{AB}}^{\alpha}(\mathbf{A}) - E_{\mathbf{AB}}^{\alpha\cup\beta}(\mathbf{A}) + E_{\mathbf{AB}}^{\beta}(\mathbf{B}) - E_{\mathbf{AB}}^{\alpha\cup\beta}(\mathbf{B}) \quad (2)$$

where $E_{\mathbf{AB}}^{\alpha}\mathbf{A}(\mathbf{A})$ is the energy of **A** in the **AB** structure calculated with the basis of **A** and $E_{\mathbf{AB}}^{\alpha\cup\beta}(\mathbf{A})$ is the energy of A in the AB structure calculated with the basis of **AB** $\alpha\cup\beta$. Correspondingly, the binding energy corrected for bsse is

$$\Delta E_{bsse} = \Delta E_b + \delta E_{CP} = E_{\mathbf{AB}}^{\alpha\cup\beta}(\mathbf{AB}) - (E_{\mathbf{A}}^{\alpha}(\mathbf{A}) + E_{\mathbf{B}}^{\beta}(\mathbf{B})) + \delta E_{\mathbf{CP}} \quad (3)$$

The interaction between two water ligands ΔE_{w-w} in the complex $(OH^-)(H_2O)_3$, has been computed as a two-body interaction using the basis set of $(OH^-)(H_2O)_3$ (in the same notation as above):

$$\Delta E_{w-w} = E_{w-w}^{(OH^-)w_3} - (E_w^{(OH^-)w_3} + E_w^{(OH^-)w_3}) \quad (4)$$

A harmonic vibrational analysis of the optimized structures was carried out using two-point differentiation of gradients[37] with a stepsize of 0.02 Å. To compare the calculated solvation energies with the experimental data, the bsse error, the vibrational zero-point (ZPE) energy correction, and the temperature corrections were taken into account. The finite-temperature corrections were estimated in the rigid rotor and harmonic oscillator approximations.[44]

Some of the structures were calculated with the hybrid HF-DFT method B3LYP as implemented in the code Gaussian94.[41] In this method the exchange-correlation energy is composed by a fraction of HF exchange combined with a fraction of the GGA exchange of Becke[4] and the entire correlation of Lee−Yang−Parr (LYP).[6]

The BOMD simulation was carried our using the Verlet integrator.[46] The time step is taken to be 10 au, i.e., 0.242 fs. A step of 10 au is employed to ensure that the velocity correlation is accurate enough for systems containing hydrogen atoms to allow calculation the vibrational spectrum, i.e., the Fourier transform of the time correlation function. The simulation was started with the constant temperature simulations which were performed by scaling the velocity at every time step so that the temperature is kept to be 300 K. Usually, the system is equilibrated about 3000 steps to eliminate possible effects of the arbitrary initial geometry. The constant energy simulations were then carried out to accumulate structural and dynamical data for 20000 time steps to calculate the statistical average of various properties.

3. Results and Discussions

3.1. Structure of $H_3O_2^-$. This is the simplest system among the aqueous clusters of the hydroxide anion, and several high-quality correlated ab initio and DFT calculations have already been reported.[22,32,33] This system is also very interesting from the point of view of validating DFT XC functionals. Geometries optimized at the MP2/aug-cc-VDZ and MP2/aug-cc-VTZ levels of theory[22,32,33] reveal a nonplanar structure with an asymmetric hydrogen bond. Table 1 contains the geometrical characteristics obtained in the present work with different XC functionals and basis sets, and compared to other DFT and post-HF results reported in the literature. Figure 1 depicts the nonplanar ground-state geometry of $H_3O_2^-$ as deduced from one of our most accurate DFT estimates (with the BLAP3 XC scheme and the Sadlej basis set). Not surprisingly, the LSD approximation failed to reproduce the asymmetry of the hydrogen bond in $H_3O_2^-$ whatever large and flexible basis sets were used. This is consistent with the known LSD overestimation of the strength of hydrogen bonds and underestimation of their lengths.[7] The GGA functional BP also fails to reproduce the asymmetry of the hydrogen bond here, although it gives relatively longer (but equal) O···H bond lengths compared to LSD. This situation remains even when very large and flexible bases are used. To verify that this is not an artifact of the auxiliary-basis fitting procedures used in deMon-KS3 for calculation of the Coulomb terms, we have made analogous tests with the BP scheme within Gaussian94[41] (denoted in Table 1 as BPg94). The results are very similar to those obtained with deMon-KS3. On the other

TABLE 1: Geometry Results for $(OH^-)H_2O$ (Distances in angstroms and Angles in Degrees)

	PLAP3	BLAP3	BP	BPg94	B3LYP	PP	LSDA	MP2[a]
R(O−H)								
Sadlej	0.968	0.964	0.976			0.978		
631++G(,*)*	*0.967*	*0.962*	*0.974*	*0.976*	*0.966*	*0.977*	*0.974*	
6311++G(*,*)	0.963	0.959			0.963	0.973		
$R(O_a-H_{2a})$								
Sadlej	0.965	0.963	0.976			0.977		
631++G(,*)*	*0.964*	*0.961*	*0.974*	*0.976*	*0.965*	*0.976*	*0.974*	
6311++G(*,*)	0.959	0.957			0.961	0.972		
$R(O_a-H_{1a})$								
Sadlej	1.097	1.158	1.227			1.190		
6311++G(*,*)	1.071	1.111			1.117	1.151		1.095
$R(O-H_{1a})$								
Sadlej	1.421	1.304	1.240			1.292		
6311++G(*,*)	1.478	1.377			1.362	1.346		1.380
$\alpha(H-O-H_{1a})$								
Sadlej	105.2	104.1	102.8			103.6		
6311++G(*,*)	106.5	104.9			106.1	104.4		
$\delta(H-O-O_a-H_{2a})$								
Sadlej	108.7	109.6	107.5			107.8		
631++G(,*)*	*108.2*	*109.4*	*106.6*	*107.6*	*109.2*	*108.4*	*109.8*	
6311++G(*,*)	106.1	107.1			109.1	107.2		
$R(O-O_a)$								
Sadlej		2.467	2.468			2.482		
6311++G(*,*)	2.5471	2.488			2.478	2.496	2.474	

[a] Optimization with MP2/aug-cc-VDZ of ref 30.

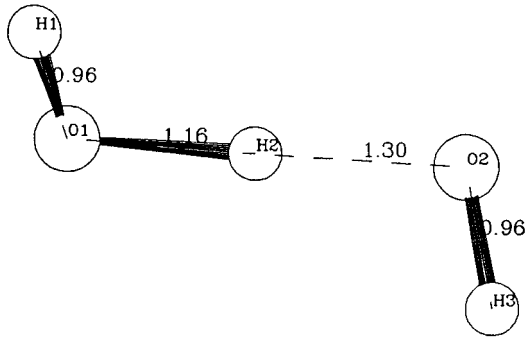

Figure 1. Structure of the complex with one water (BLAP3 functional).

hand, the GGA XC scheme Perdew−Perdew yields an asymmetric hydrogen bond in $H_3O_2^-$ as is seen from Table 1 ($R(O_a-H_{1a})$, the shorter bond, $R(O-H_{1a})$, the longer bond). Therefore, the type of exchange functional used is of particular importance in this respect. This fact is reconfirmed by comparing the BLAP3 with the PLAP3 results: both give an asymmetric geometry of the hydrogen bond bridge close to the MP2 estimates, but the degree of asymmetry (shorter vs longer O···H bond) is stronger when the exchange functional of Perdew is used (as in PLAP3). The results for the longer hydrogen bond are particularly important: GGA and (to a lesser extent) MP2 tend to shorten such weak O···H bonds.[1,12]

Besides the type of XC functional used, the choice of the basis set has a noticeable impact on the results, especially for the hydrogen-bond geometry. The influence of the basis set is clearly demonstrated in Tables 1 and 2, comparing the results obtained with 631++G(*,*), 6311++G(*,*), and with the exhaustive basis set of Sadlej.[39] The BLAP3/6311++G(*,*) and PLAP3/Sadlej estimates of the hydrogen-bond lengths in $(OH^-)H_2O$ are the closest to the MP2/aug-VDZ values.[32,33] A geometry of similar quality is obtained with the hybrid B3LYP XC scheme (Table 1). Including diffuse functions in the basis is required by the low-barrier nature of the hydrogen bond here and the fact that the potential energy surface is very flat with respect to the hydrogen-bond degrees of freedom. Switching from 631++G(*,*) to 6311++G(*,*) bases leads to a noticeable shortening of the (shorter) O_a-H_{1a} bond and elongation of the longer hydrogen bond for most of the methods used.

We should point out that the O−proton bond length may be sensitive to other factors, for example, the starting geometry guess. This is a result of the extreme flatness of the potential energy surface. We were able to obtain two different minima using a Sadlej basis set and the PP functional. The energy difference between these two geometries is only 0.00163 kcal/mol. while the O−proton and proton−O distances are 1.230, 1.245 and 1.190, 1.292 Å, respectively.

It is worth noticing that getting the right geometry of the isolated OH^- ion is also not an easy task for DFT. The LAP XC schemes give here a relatively better bond length than the other XC functionals referred to in Table 2. Negative ions of this type are known to be difficult cases for approximate XC functionals, and for ab initio treatments in general.[20,21,49]

Our calculations confirm the observation of ref 33 that the angle $H-(O-O_a-H_{2a})$, Figure 1, (the angle β in ref 33) and the angle $H-O-H_{1a}$ are very sensitive to the XC functional and basis set used, as these angles are related to the geometry of the hydrogen bond in $(OH^-)H_2O$. As in the case of the O−proton distances, the static values of these angles should not be taken too literally as the proton moves almost freely between the two oxygens.

Concerning the binding energy at T = 0 K (ΔE_b^e) and the binding enthalpy at 298 K of $H_3O_2^-$, the results of the different XC schemes are presented in Table 3. The energies are corrected for the bsse using the counterpoise (CP) method (the bsse corrections are given in parentheses). The largest CP corrections occur with the TZVP+ basis, about 4−5 kcal/mol, which is comparable to the CP corrections reported with MP2 with the 6311++G(*,*) basis set.[33,20] The KS-DFT methods are less bsse demanding compared to MP2, and with the exception of TZVP+, the rest of the bases used in our study lead to relatively smaller CP corrections, about 1−2 kcal/mol (Table 3).

We also did calculations with the LSD scheme (VWN correlation[45]) just to reconfirm the significant overestimation

TABLE 2: Geometry of OH^- with Different Methods (Distances in angstroms)

	B3LYP/A[a]	B3P86/A	BHLYP/A	BLYP/A	BP86/A	BP86/631	exptl[a]
R(O−H)	0.974	0.972	0.961	0.986	0.984	0.9795	0.964
	BP/631++	BL3/631++	PL3/631++	BP/Sadlej	BL3/Sadlej	PL3/Sadlej	
R(O−H)	0.9795	0.967	0.970	0.981	0.968	0.971	

[a] A denotes the basis used in ref 49.

TABLE 3: Energetics (kcal/mol) of $(OH^-)H_2O$. bsse Correction (when Available) in Parentheses below the Energy Including It

	PLAP3	BLAP3	BP	BPg94	PP	B3LYP	MP2	CCSD(T)//MP2
ΔE_b^e(0 K)								
Sadlej	−24.2	−24.4	−28.6		−30.2			
	(0.99)	(0.99)	(0.9)					
631++G(,*)*	−25.3	−25.6	−29.5	−29.8	−30.1	−28.6	−24.2[a]	
	(1.9)	(1.8)	(1.9)	(2.0)	(2.0)	(1.6)		
6311++G(*,*)	−24.5	−24.6				−27.8	−24.1[a]	
	(1.9)	(1.9)				(1.6)	(4.24)[a]	
aug-cc-VDZ						−27.4	−26.8[b]	−24.6[c]
						(0.4)		(2.3)
TZVP+	−24.9	−25.3	−29.7			−28.6		
	(4.5)	(4.2)	(4.2)			(3.6)		
ΔH_b°(298 K)								
Sadlej	−24.5	−25.8	−30.4					
631++G(,*)*	−25.7	−26.6	−31.1			−29.3	−28.6[b]	
6311++G(*,*)	−24.8	−25.5				−28.3	−24.4[a] (−28.6[b])	
aug-cc-VDZ						−27.9	(−27.0[b])	
exptl ΔH_b (T = 300 K)		−25.0[d]			−26.5 ± 1.0[e]			

[a] MP2/6311++G(*,*) bsse corrected results of ref 17. [b] MP2/aug-cc-DVZ results of ref 30 without bsse corrections. [c] CCSD(T)/augcc-DVZ//MP2 results of ref 17 with bsse correction. [d] Experimental data from ref 22. [e] Experimental data from ref 21.

of the hydrogen bond energy this method gives: about −40.0 kcal/mol without bsse corrections and about −38.2 kcal/mol with the CP correction with the 631++G(*,*) basis. Using bigger bases does not improve the situation much.

It should be mentioned that the experimentally derived estimate of ΔE_b^e(0 K) is about −26.0 ± 1.0 kcal/mol (after subtracting from the measured enthalpy at 298 K the average finite-temperature plus ZPE correction of about −0.5 kcal/mol as estimated from the MP2, B3LYP, and LAP results). Considering the GGA results, the bsse corrected binding energy obtained with BP (Sadlej basis) is −28.6 kcal/mol, slightly above the upper limit of the experimental error bar for ΔE_b^e(0 K) (about −27.0 kcal/mol). We repeated the BP calculation with Gaussian94 (BPg94 in Table 3) using the same basis (631++G(*,*)), which gave a binding energy close to the BP value obtained with deMon-KS3 with a difference of about 0.3 kcal/mol. The GGA scheme PP gives slightly larger overbinding than the BP functional, a similar trend is seen for water clusters and positively charged hydrated proton clusters.[16] The hybrid B3LYP scheme leads to a slight improvement over GGA, giving a bsse corrected binding energy of −27.8 kcal/mol with the 631++G(*,*) basis, and −27.4 kcal/mol with the aug-cc VDZ basis, very close to the upper limit of the experimental error bar. In contrast to GGA and B3LYP, the LAP XC schemes yield (bsse corrected) binding energies near the lower limit of the experimental bar for ΔE_b^e(0 K) of about −25.0 kcal/mol (Table 3): −24.4 kcal/mol with BLAP3/Sadlej, and −24.2 kcal/mol with PLAP3/Sadlej. The benchmark CCSD(T)//MP2-augcc-VDZ estimate of ΔE_b^e(0 K) reported by Grimm et al.[33] gives about 24.6 kcal/mol with aug-cc-pVDZ basis (after the bsse correction of about 2 kcal/mol was taken into account) which is also very close to and supports the lower limit of the experimental bar for the binding energy. Having a high quality energy estimate here is very important in view of the large error bar of the experimental measurements. The bsse-corrected MP2/6311++G(*,*) estimate of ΔE_b^e(0 K). ≈−24.1 kcal/mol reported by Grimm[33] is also very close to the CCSD(T)/aug-cc-VDZ estimate, showing that the bsse correction at the MP2 level is significant for these systems (such a correction is missing in the MP2/aug-cc-VDZ results of ref 32, which obscures the assessment of these results).

Taking into account the bsse, ZPE and temperature corrections at 298K with the B3LYP hybrid scheme leads to an enthalpy of association of −27.9 kcal/mol with aug-cc-VDZ basis and −28.3 kcal/mol with the 6311++G(*,*) basis set, which is about 0.5 kcal/mol more negative than the zero temperature vibrationless limit ΔE_b^e (Table 3), and slightly above the upper limit of the experimental bar for $\Delta H°$(298 K) (about −27.5 kcal/mol). Unfortunately, bsse-corrected MP2 energies are reported only at T = 0 K.[33]

The BLAP3 and PLAP3 estimates for the enthalpy of association of one water are −24.5 kcal/mol and −25.8 kcal/mol respectively with the Sadlej basis, and are close to the lower end of the experimental bar of about −25.5 kcal/mol. With the 6311++G(*,*) basis both LAP schemes give enthalpy values within the experimental error bar, close to the center, −26.5 kcal/mol. It should be noted that the ZPE and the finite-temperature binding energy corrections tend to cancel each other to a large extent for this system, in agreement with the MP2 results reported previously:[32,33] overall, the value of $\Delta H°$(298 K) only slightly exceeds the corresponding zero temperature vibrationless limit ΔE_b^e by about 0.3 to 0.7 kcal/mol with PLAP3, B3LYP, and MP2, and by about 1 kcal/mol with BLAP3.

Finally, we have tried to estimate the energy barrier for proton transfer in $H_3O_2^-$. The large basis set MP2/augcc-VDZ estimate of Xantheas[32] yields a very small value for this barrier, about 0.3 kcal/mol. The nonplanar transition state structure with the proton placed symmetrically in the middle of the hydrogen bond is very close in energy to the asymmetric minima, and the ZPE contribution (of about the same magnitude as the energy barrier) may lead to an almost barrierless movement of the proton

TABLE 4: Energy Barrier for PT [kcal/mol] in $(OH^-)H_2O$

	PLAP3	BLAP3	B3LYP	MP2[a]
$\Delta E^{\ddagger}$				
631++G(*,*)	0.47	0.06	0.02	
aug-cc-DZV			0.09	0.50

[a] MP2/aug-cc-VDZ result of ref 30.

between the two oxygens. Table 4 contains our results for the PT energy barrier with different basis sets and methods. It is seen that the value is very sensitive to both the method and the basis set: PLAP3 yields a PT energy barrier of about 0.4 kcal/mol comparable to the MP2 estimate of about 0.3 kcal/mol.[32] BLAP3 and B3LYP give much smaller (almost vanishing) values, 0.06 and 0.02 kcal/mol respectively, which points out also the importance of the exchange functionals used: as mentioned above, the XC schemes involving the GGA exchange of Becke tend to give less asymmetric hydrogen bonds, which is reflected in the lower PT energy barriers obtained with these XC schemes.

3.2. Structure of $(OH^-)(H_2O)_2$ and $(OH^-)(H_2O)_3$. The complex of OH^- with two water ligands ($n = 2$) is quite a demanding task for theoretical studies. The large basis set MP2 calculations of Xantheas[32] and Grimm[33] gave somewhat overestimated binding energies for this system. As we found in the one-water case, the basis set of Sadlej seems to provide a sufficient accuracy for our DFT calculations. To verify the basis set influence in this case, we present results with the 631++G(*,*) basis as well. The hybrid B3LYP estimates obtained with Gaussian94 are also given for comparison in the case of $n = 2$, Table 5. Table 6 contains the calculated structural parameters in the case of three water ligands ($n = 3$). The geometry of these two aqueous complexes is depicted on Figures 2 and 3.

The comparison of the results for $n = 2$ and $n = 3$ with those for the one water case (Table 1) shows that with increasing number of water ligands, the $OH^- - H_2O$ interaction becomes more like a normal hydrogen bond, instead of a low-barrier (strong) hydrogen bond. This is clear from the thermodynamic data for hydration. If we consider the results of PLAP3 with the Sadlej basis set; for example, the hydration enthalpies are −24.5, −17.9, and −14.4 for one, two, and three waters, respectively, which is very similar to the result for hydration of hydronium (H_3O^+).[16] The large value of the hydration enthalpy is partly due to the presence of negative charge. Similar to the case of hydronium, the hydration enthalpy here approaches the value typical for a water cluster when the size of the solvated OH^- becomes sufficiently large. As the hydrogen bonds between $OH^-\cdots H_2O$ tend to enlarge, the stretching of the covalent O−H bonds respectively decreases. In other words, the asymmetry of the O−H···O structure becomes larger compared to the case of one water. The PLAP3 scheme and MP2 both yield here hydrogen bonds with somewhat larger asymmetry (the shorter $R(O_a-H_{1a})$ vs the longer $R(O-H_{1a})$ in Tables 5 and 6) compared to BLAP3, which in turn gives slightly more asymmetric structures than B3LYP. In contrast to the case of $n = 1$, the GGA functional BP gives here also asymmetric hydrogen bonds, but less pronounced than the other methods. Overall there is a good agreement between the BLAP3, PLAP3 (deMon-KS3) and B3LYP (Gaussian94) geometry estimates. As in the case of $n = 1$, PLAP3 tends to give slightly longer hydrogen bond lengths compared to MP2, BLAP3 and B3LYP. One should keep in mind (in the absence of any experimental geometry data) that MP2 is not always a perfect guide, as it sometimes tends to shorten intermolecular hydrogen bonds involving O and H atoms.[1,12] In the case of $n = 2$, a somewhat larger difference between DFT and MP2 occurs in the estimation of the angle O_a-O-O_b and the related distance $O_a\cdots O_b$. The BLAP3 and PLAP3 schemes yield larger values for the O···O···O angle

TABLE 5: Geometry of $(OH^-)(H_2O)_2$ with Different Methods (Distances in angstroms and Angles in Degrees)

	PLAP3	BLAP3	BP	B3LYP	MP2/aug-cc-VDZ[a]
R(O−H)					
Sadlej	0.966	0.963	0.975		
631++G(,*)*	*0.965*	*0.962*	*0.973*	*0.966*	
aug-cc-VDZ				0.964	0.967
$R(O_a-H_{1a})$					
Sadlej	1.038	1.041	1.071		
631++G(,*)*	*1.035*	*1.038*	*1.061*	*1.040*	
aug-cc-VDZ				1.039	1.038
$R(O-H_{1a})$					
Sadlej	1.563	1.533	1.481		
631++G(,*)*	*1.570*	*1.537*	*1.498*	*1.531*	
aug-cc-VDZ				1.538	1.543
ä(H−(O−O_a−H_{2a})					
Sadlej	115.9	117.4	109.21		
631++G(,*)*	*114.5*	*117.4*	*119.19*	*113.3*	
aug-cc-VDZ				109.0	118.1
á(O_a−O−O_b)					
Sadlej	128.4	126.9	133.44		
631++G(,*)*	*123.7*	*123.0*	*127.88*	*119.3*	
aug-cc-VDZ				132.2	115.6
$R(O_b-H_{1b})$					
Sadlej	1.033	1.038	1.063		
631++G(,*)*	*1.032*	1.036	*1.062*	*1.045*	
aug-cc-VDZ				1.041	1.033
$R(O-H_{1b})$					
Sadlej	1.571	1.543	1.502		
631++G(,*)*	*1.583*	*1.550*	*.493*	*1.515*	
aug-cc-VDZ				1.532	1.559
ä(H−O−O_b−H_{2b})					
Sadlej	127.8	112.8	109.42		
631++G(,*)*	*113.9*	*111.5*	*107.60*	*110.1*	
aug-cc-VDZ				113.4	109.2
$R(O_a-O_b)$					
Sadlej	4.685	4.610	4.700		
631++G(,*)*	*4.593*	*4.530*	*4.588*	*4.420*	
aug-cc-VDZ				4.705	4.375

[a] Optimization with MP2/aug-cc-VDZ of ref 30.

TABLE 6: Geometry of $(OH^-)(H_2O)_3$ with Different Methods (Distances in angstroms and angles in degrees)

	PLAP3	BLAP3	BP	MP2/VDZ(pyramidal)[a]
R(O−H)				
Sadlej	0.966	0.963	0.974	0.964
631++G(,*)*	*0.965*	0.961	*0.974*	
α(H_{2a}−O_a−H_{1a})				
Sadlej	101.8	103.0	102.40	99.7
631++G(*,*)	*102.9*	*102.9*	*102.24*	
$R(O_a-H_{2a})$				
Sadlej	0.964	0.961	0.972	0.967
631++G(,*)*	*0.963*	0.960	*0.972*	
$R(O_a-H_{1a})$				
Sadlej	1.011	1.018	1.034	1.008
$R(O-H_{1a})$				
Sadlej	1.668	1.614	1.589	1.656
$R(O_a-O_b)$				
Sadlej	4.726	4.354	4.274	3.321
$R(O_b-O_c)$				
Sadlej	4.458	4.458	4.340	
$R(O_c-O_a)$				
Sadlej	3.730	4.388	4.340	
α(O_a−O−O_b)				
Sadlej	125.2	111.1	110.0	78.1
631++G(,*)*	*106.7*	*108.5*	*109.31*	

[a] Optimization with MP2/aug-cc-VDZ of ref 30.

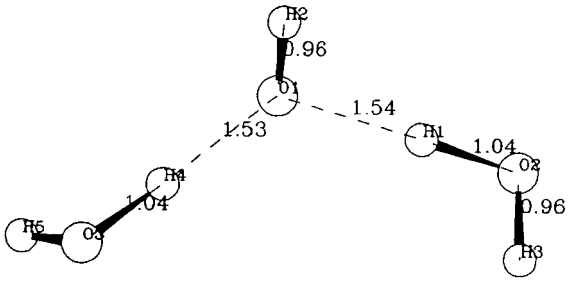

Figure 2. Structure of the complex with two waters (BLAP3 functional).

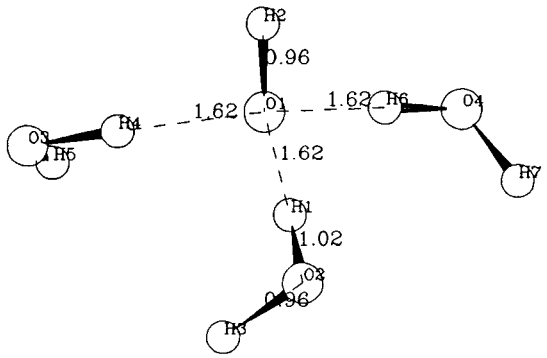

Figure 3. Structure of the complex with three waters (BLAP3 functional).

(about 126.9° and 128.4°, respectively, with the Sadlej basis and about 123.0 and 123.7 with 631++G(*,*)), compared to the MP2/aug-cc-VDZ estimate of about 115.6. The B3LYP/631++G(*,*) and B3LYP/augcc-VDZ estimates are somewhat between, giving about 119.3° and 132.2°, respectively, for this angle. The GGA BP/Sadlej estimate of the same angle is about 133.4°. The difference in the results for the O···O···O angle leads to a difference in the distance between the two ligand oxygens O_a-O_b: about 4.6 Å with the LAP schemes vs the MP2 estimate of about 4.38 Å The B3LYP estimate of this distance shifts substantially with increasing basis set size, from 4.42 Å with the 631++G(*,*) basis to about 4.7 Å with the aug-cc-VDZ basis, the latter being close to the LAP/Sadlej estimates (Table 5).

Comparing the BLAP3 and PLAP3 results with B3LYP the overall agreement for the geometry data is good, with the exception of the controversial angle O···O···O, and the angles $\delta(H-O-O_a-H_{2a})$ and $\delta(H-O-O_b-H_{2b})$. The influence of the basis set on most of the other geometry parameters is small (Table 5). A similar situation is observed with the geometry of the complex with three waters (Table 6). Again the overall agreement between DFT (LAP) and MP2 is good with the exception of the O···O···O angles, and the corresponding O···O distances, where differences similar to the case of $n = 2$ occur. This leads to differences in the overall shape of the complex, comparing the LAP with the MP2 structures. The MP2 geometry optimization of Xantheas[32] was performed under a C_3 symmetry constraint, whereas our DFT calculations were performed without any constraint. We have recomputed the MP2 geometry using the same basis set as Xantheas, with and without a symmetry constraint. The relaxation of the optimized structure from C_3 to C_1 did not change too much the MP2 geometry results. The BLAP3 and PLAP3 functionals give here O···O···O angles about 108.5° and 106.7°, respectively, which is close to a tetrahedral geometry of the complex. The MP2 estimate of these angles is about 78°, which seems too small in view of possible steric effects of the water ligands. A quasi-tetrahedral geometry of the aqueous complex with three waters seems to us more logical since with three waters all the central oxygen lone pairs are involved in bonding. It should be pointed out here that both MP2 and DFT (LAP) estimates indicate a slightly attractive water−water (ligand−ligand) interaction of about 0.5 kcal/mol.

It is worth comparing the binding energies for successive hydration. Table 7 contains the results for the total binding energy $\Delta E_b^e(0\ K)$ for $n = 2$ and the binding energy of successive association, as well as the corresponding enthalpies at 298 K. The bsse and ZPE corrections were taken into account, with a few exceptions due to a lack of literature data. The BLAP3/Sadlej and PLAP3/Sadlej estimates of the enthalpy of association of $(OH^-)(H_2O)_2$ are slightly below the center of the experimental error bar of about −17.6 kcal/mol. With the 6311++G(*,*) basis the LAP enthalpy remains very close to the results with the Sadlej basis within a slight increase of about 0.7 kcal/mol. All other methods tend to overestimate the binding enthalpy for $n = 2$: MP2 by about 1−2 kcal/mol, B3LYP by about 2−3 kcal/mol and GGA BP by about (3−4 kcal/mol). As mentioned above, the only MP2 result available for the enthalpy (from ref 32) was not corrected for bsse, which brings an uncertainty of about 2−5 kcal/mol.

Turning to the binding enthalpy of $(OH^-)(H_2O)_3$ (Table 8), the MP2 results reported in the literature are close to the upper limit of the experimental error bar for $(\Delta H°)_{3,2}$,[32] but we again point out that these were not corrected for bsse. The bsse-corrected MP2 results of Grimm[33] were reported only for the zero temperature limit. Our bsse-corrected BP/Sadlej value of $(\Delta H°)_{3,2}$ is in fact in very good agreement with experiment, close to the upper limit (about −17.1 kcal/mol) of the experimental error bar. The PLAP3/Sadlej and BLAP3/Sadlej estimates are, in turn, slightly below the lower end of the experimental error bar, which is about −15.1 kcal/mol (Table 8).

Summarizing the performance of the different methods, the LAP schemes seem overall to give slightly improved results for the aqueous complexes with one and two waters, compared to the BP, MP2, and B3LYP estimates. For $n = 3$ the BP/Sadlej energy estimate is slightly better than the LAP/Sadlej and MP2/aug-cc-VDZ estimates (B3LYP results have not been reported for this case), the latter having the uncertainty of the uncorrected bsse. The decrease of the binding energy of successive association is well reproduced by all the methods used. This effect can be explained as partly due to direct ligand−ligand interactions, partly due to nonadditive (cooperative) effects of interaction between the hydrogen bonds. The O···H bond strength decreases as more water is added to the OH^- hydrates and the O···H bond lengths become longer, respectively. The main reason is that the negative charge on the OH^- group is distributed between a larger number of hydrogen bonds when the number of water ligands increases.

3.4. Frequency Analysis. Vibrational analysis of hydrogen bonded systems gives valuable additional insight into the nature of hydrogen bonding, especially if there is reliable experimental data to match. It is useful to compare first the different methods for the vibrational frequency of isolated OH^- (Table 9). The experimental value for the harmonic frequency (ω_e) and anharmonic correction($\omega_e\ x_e$) are, 3738.44 and 91.42 cm^{-1},[50] respectively. The BLAP3 (631++G(*,*)) frequency is 3728.8 cm^{-1} which is close to the MP2 value of 3767 cm^{-1} and somewhat larger than the PLAP3 estimate of 3670.8 cm^{-1}. To obtain the anharmonic correction to the harmonic frequency of OH^- we have calculated the potential energy curve with the

TABLE 7: Energetics (kcal/mol) of $(OH^-)(H_2O)_2$. bsse Correction (when Available) in Parentheses below the Energy Including It

	PLAP3	BLAP3	BP	PP	B3LYP	MP2/aug-cc-VDZ[a]	MP2/DVP(s,p)[b]
(ΔE_b^e(0 *K*))							
Sadlej	−44.2	−44.1	−49.9	−53.9			−45.8
(1.8)	(1.8)	(1.6)	(6.3)				
631++G(,*)*	*46.0*	*−46.0*	*−54.3*	*−50.7*			
(3.3)	(3.3)	(3.0)	(3.0)				
aug-cc-VDZ					−49.6	−49.0	
$(\Delta E_b^e)_{2,1}$(0 K)							
Sadlej	−19.9	−19.7	−21.3	−23.6			−21.2
(0.9)	(0.8)	(0.5)	(3.2)				
631++G(,*)*	*−20.7*	*−20.4*	*−24.7*	*−22.1*			
(1.4)	(1.5)	(1.2)	(1.3)				
aug-cc-VDZ						−22.1	
$(\Delta H_b)_{2,1}$(298 K)							
Sadlej	−17.9	−17.0	−18.6				
631++G(*,*)	−18.6	−17.8	−21.9				
aug-cc-VDZ						−20.1[a]	
exptl $(\Delta H_b)_{2,1}$(300 K)		−16.4[c]		17.6 ± 1.0[d]			

[a] MP2/aug-cc-VDZ results of ref 30 not corrected for bsse. [b] MP2/DVP(s,p) results of ref 31, corrected for bsse. [c] Experimental data from ref 22. [d] Experimental data from ref 21.

TABLE 8: Binding Energy in kcal/mol for $(OH^-)(H_2O)_3$

	PLAP3	BLAP3	BP	PP	MP2/aug-cc-VDZ[a]	MP2/DVP(s,p)[b]
ΔE_b^e(no bsse correct.)						
Sadlej	−63.5	−63.2	−69.7	−73.9	−68.5	−71.1
631++G(,*)*	*−68.1*	*−67.7*	*−78.6*			
ΔE_b^e(with bsse correct.)						
Sadlej	−60.7	−60.6	−67.7			−63.0
631++G(,*)*	*−63.5*	*−63.2*	*−74.7*			
$(\Delta E_b^e)_{3,2}$(no bsse correct.)						
Sadlej	−17.4	−17.3	−18.3	−20.0	−19.5	−19.0
631++G(,*)*	*−18.8*	*−18.4*	*−21.3*			
$(\Delta E_b^e)_{3,2}$(with bsse correct.)						
Sadlej	16.5	16.5	17.8		−17.2	
631++G(,*)*	*−17.5*	*−17.2*	*20.5*			
$(\Delta H_b)_{3,2}$(298 K)						
Sadlej	−14.4	−14.4	−15.5			
631++G(,*)*	*−15.4*	*−15.1*	*−18.3*		*−16.9*[a]	
expt. ΔH_b(300 *K*)		−16.1 ± 1.0[c]				

[a] MP2/aug-cc-VDZ results of ref 30 not corrected for bsse. [b] MP2/DZP(s,p) results of ref 31, corrected for bsse. [c] Experimental data from ref 21.

TABLE 9: Vibrational Frequency of OH^- in cm^{-1}

	PLAP3	BLAP3	BP	B3LYP	PP	exptl	MP2 [2]
R(O−H)							
631++G(,*)*	*3670.8*	*3728.8*	*3663.9*				
aug-cc-VDZ	3695.3					3738.4	3767.0

[a] Reference: Xantheos, S. S. *J. Am. Chem. Soc.* **1995**, *117*, 10373, optimization MP2/aug-cc-VDZ. [b] Optimization MP2/aug-cc-VTZ.

BLAP3/(631++G(*,*) functional and have made a least-squares fit to the Morse potential:[51]

$$V = D_e(1 - \exp(-B_e q))^2 \qquad (5)$$

where q is the vibrational coordinate, $q = r - r_e$, r_e is the equilibrium bond length. We obtained $D_e = 39532.5$ cm^{-1} (BLAP3), and $B_e = 1.1876$ $bohr^{-1}$. This leads to a harmonic frequency of 3761.4 cm^{-1} (which is a little different from the value of 3728.8 cm^{-1} calculated by a straight quadratic fit) and anharmonic correction of 89.4 cm^{-1}. The latter is in excellent agreement with the experimental estimate of 91.4 cm^{-1}, which is good news for the BLAP3 functional validation. Concerning the frequencies of the isolated water all the methods give more unified estimates (Tables 10 and 11).

To our knowledge, there is no experimental data reported to date for larger hydrated OH^- clusters. We calculated the vibrational frequencies for all optimized structures using methods and basis sets discussed in previous sections. The results for BLAP3 with the 631++G(*,*) basis set are shown in Table 10 as an example. The stretching modes corresponding to the covalent O−H bonds are clearly distinguished − above 3700 cm^{-1} in Table 10, originating from the parent O−H stretches in H_2O. A slight red shift is obtained, more noticeable with BLAP3 and PLAP3. The agreement between the different methods is overall very good for these modes. For $OH-H_2O$, the mode associated with proton motion is in the range of 600−1300 cm^{-1} and sensitive to the method and basis set used. For example, using 631++G(*,*) basis set, we obtained, 656, 768, 1053,1090, and 1300 cm^{-1}, for BP, PP, B3LYP, BLAP3, and PLAP3, respectively. The B3LYP and BLAP3 results are very close to each other for these modes, and somewhat different from PLAP3. The latter gives frequencies closer to (but still different from) the MP2 estimates. These differences should be related to the different results for the hydrogen bond geometry, as discussed in the previous section: the XC schemes involving the GGA exchange of Becke (BLAP3, BP) tend to give more symmetric hydrogen bond structures, which is related to the observed relatively smaller values of the corresponding frequency, compared to the PLAP3 and MP2 estimates. As a result of the large amplitude motion of the proton, there should

TABLE 10: Harmonic Vibrational Frequencies in cm^{-1} for OH^- H_2O and OH^- $(H_2O)_n$ (n = 1−3), BLAP3 631++G(*,*)

OH^-	H_2O	$OH^-(H_2O)$	$OH^-(H_2O)_2$	$OH^-(H_2O)_3$
3729	1629	189	27	32
	3823	301	101	34
	3946	501	155	55
		601	275	135
		1090	280	141
		1414	327	190
		1668	487	249
		3804	545	280
		3837	601	285
			1169	438
			1191	441
			1700	508
			1710	563
			2377	568
			2566	1069
			3833	1086
			3866	1089
			3867	1693
				1724
				1725
				2798
				2808
				2972
				3842
				3875
				3876
				3877

TABLE 11: Harmonic Vibrational Frequencies in cm^{-1} for OH^- H_2O and $OH^-(H_2O)_n$ (n = 1−3), B3LYP 631++G(*,*) and MP2/aug-cc-VDZ

OH^-		H_2O		$OH^-(H_2O)$		$OH^-(H_2O)_2$		$OH^-(H_2O)_3$
B3LYP	MP2	B3LYP	MP2	B3LYP	MP2	B3LYP	MP2	B3LYP
3729	3767	1601	1623	187	207	29	18	42
		3805	3805	295	328	106	99	45
		3927	3940	503	453	167	161	241
				586	570	288	283	298
				1053	1321	305	306	329
				1428	1608	344	345	348
				1662	1729	477	454	469
				3812	3814	550	542	529
				3839	3864	605	575	538
						1181	1138	970
						1201	1163	980
						1698	1690	1712
						1708	1703	1717
						2360	2453	3029
						2564	2642	3177
						3838	3834	3829
						3861	3876	3832
						3862	3878	3870

be a noticeable vibrational anharmonicity for the modes associated with its movement.[16] The results presented in Tables 9−11 do not yet include anharmonicity, a matter discussed in the next section. The group of low-frequency modes below 500 cm^{-1} originate from collective-deformation and collective bending modes, and we find a very good agreement between all the methods for these modes.

It is interesting to compare these results with the frequencies of hydrated proton clusters. It is believed that the signature proton vibrational frequency is about 1000 cm^{-1} [16,52] for $H_5O_2^+$ (PP functional and DZVP basis set). The corresponding frequency in the case of $H_3O_2^-$ using the Sadlej basis set and the same PP functional is about 746.8 cm^{-1}. The corresponding BP value is about 656.2 and 611.6 cm^{-1} with 631++G(*,*) and the Sadlej basis sets, respectively. This frequency shift should be associated with the widening of the flat potential energy surface between the two oxygen atoms in $H_3O_2^-$, at least

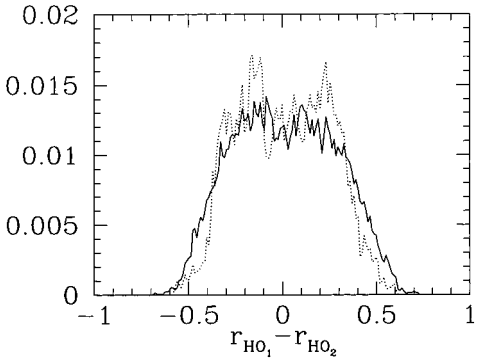

Figure 4. Population profile of proton obtained by BOMD simulation for $OH-H_2O$ using the PP (solid curve) and BP86 (dotted curve) functionals. The *X*-axis (in angstroms) is a measure of the deviation of the proton's position from the center of the O_1-O_2 bond.

when using GGA functionals. As we indicated earlier, the proton in $H_3O_2^-$ moves in a larger area between the two host oxygens, compared to the situation in $H_5O_2^+$, and essentially experiences no energy barrier according to the GGA estimates.

It is apparent that the signature proton frequency in $H_5O_2^+$ and in $H_3O_2^-$ are quite different even if the same functional and basis set are used. This fact remains to be verified by experimental data. It is worth repeating that the calculated results depend quite noticeably on the methods and basis sets used for $H_3O_2^-$. Such a strong dependence was not observed for $H_5O_2^+$. In the case of $OH-(H_2O)_2$ and $OH-(H_2O)_3$, the frequencies associated with the proton motion increase rapidly to 2000−3100 wavenumbers. Clearly the protons behave here more or less like tightly bound hydrogens. It is interesting to note that the stretch frequencies of the water molecule increase when the cluster size becomes larger. Eventually it tends to approach the frequency of the free water molecule(gas phase), a reflection of the fact that the covalent O−H bond is less influenced by the presence of charge and other species. This trend is shared by hydrated proton clusters.[16]

3.5. BOMD Simulation. Given the flatness of the energy surface for proton motion in the $(OH^-)H_2O$ system, thermal fluctuations represent an important factor in determining the landscape of the free energy surface and the dynamics of proton transfer. We have developed an ab initio BOMD technique[16] which can be used to study dynamics and structure at finite temperature. The simulation was carried out for $(OH^-)H_2O$ using the 631++G(*,*) basis set with the GGA-BP functional and the Sadlej basis set with the GGA-PP functional at 300 K.

The population analysis obtained by BOMD simulation is shown in Figure 4. The *X*-axis is a measure of the deviation of the proton's position from the center of the O_1-O_2 bond, i.e., $r_{HO_1} - r_{HO_2}$. We observe a very broad peak ranging from −0.5 to 0.5 Å. It is, in fact, much broader than that in the case of $H_5O_2^+$. It is interesting to note that the BP and PP profiles are very similar here, while at 0 K these two functionals yield quite different structures: BP gives a symmetrical structure with the proton equally shared by the two oxygens, while PP gives an unsymmetrical one with the proton closer to one of the oxygens (O_1-H, 1.19 Å and O_2-H, 1.29 Å). As we indicated earlier, yet another, more symmetrical, structure was obtained with PP, at an energy difference of only about 0.00163 kcal/mol. What we see here is that, because of the extremely flat energy surface, the thermal motion can easily overcome all the barriers to allow the proton to move more or less freely in a large area between the two oxygen atoms. Therefore one should not lend undue importance to the optimized O−proton distance. Let us note that the population is related to the mean force potential by a

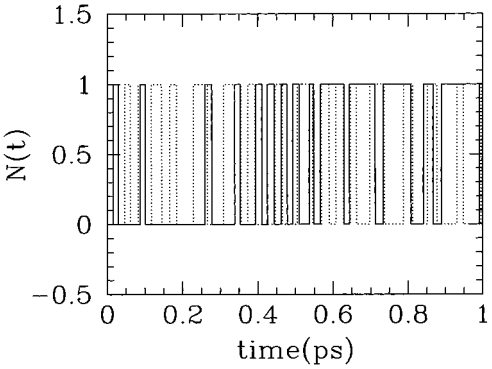

Figure 5. Plot of the transition counting function $N(t)$ as a function of time. The solid and dotted lines are results of PP and BP86 functionals, respectively.

simple logarithmic transformation and hence is considered as equivalent to the relative free energy. Therefore, the relative free energy profile of the proton obtained with PP and BP are very similar, and the free energy is of a single-well type, without any apparent barrier. This seems to be a typical free energy situation for system with a strong hydrogen bond.[53]

The proton-transfer dynamics can be well described by a transition counting autocorrelation function[47]

$$C(t) = \frac{\langle \delta N(t) \delta N(0) \rangle}{\langle \delta N(0) \delta N(0) \rangle} \tag{6}$$

where $\delta N(t) = N(t) - \langle N \rangle$, $N = 1$ if the O−proton distance is less than half of the O−O distance, otherwise, $N = 0$; $\langle N \rangle$ is the statistical average representing the probability of finding the proton on the left of the O−O midpoint. Theoretically it should be equal to 0.5 when the simulation is long enough. If the transition is a first-order process, we have

$$\frac{N(t)}{dt} = -k_f N(t) + k_b N'(t) \tag{7}$$

where $N'(t)$ is the corresponding instant transition counting function for a proton on the right side of the middle point, i.e., the reverse process, k_f and k_b are the forward and backward rate constants, respectively. The decay of $N(t)$ is exponential with a time constant of $(k_f + k_b)^{-1}$. The short time behavior of $C(t)$ is also an exponential with a time constant of τ:

$$C_s(t) = \exp\left(\frac{-t}{\tau}\right) \tag{8}$$

where

$$\tau = \frac{1}{k_f + k_b} \tag{9}$$

There is an equilibrium relation between k_f and k_b

$$\frac{\langle N \rangle}{1 - \langle N \rangle} = \frac{k_b}{k_f} \tag{10}$$

We then obtain

$$k_f = \frac{1 - \langle N \rangle}{\tau} \tag{11}$$

Figure 5 shows the transition pattern of the shared proton, i.e., $N(t)$ as a function of time. The proton transfer occurs on a subpicosecond time scale. This may be a result of the low barrier

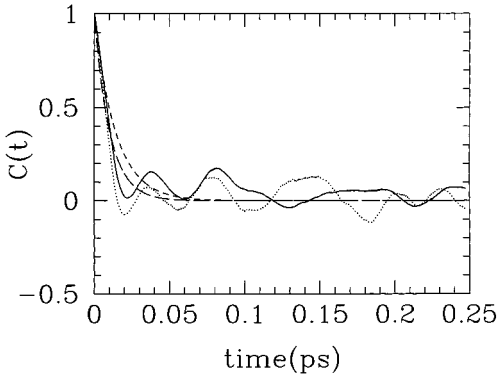

Figure 6. Plot of the transition counting autocorrelation function as a function of time. The solid and dotted lines are results of PP and BP86 functionals, respectively. The long and short dashed lines are the corresponding exponential fitting functions.

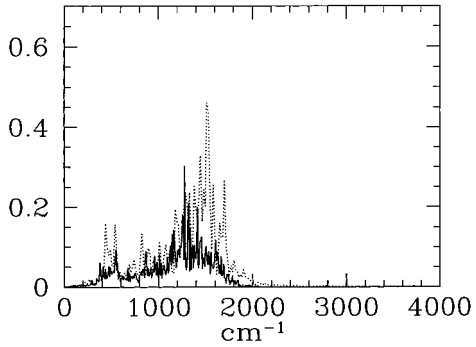

Figure 7. Plot of the vibrational spectra due to proton motion calculated by the BOMD simulation. The solid and dotted lines are results of PP and BP86 functionals, respectively.

height, at least as represented by the functionals used. It is believed that the proton hopping time is in the range of 1 ps in the liquid state.[48] Comparing the PP result with the BP estimate, clearly, the proton transfers more frequently when the BP functional is used. It is a reflection of the fact that the proton-transfer barrier is lower with BP than with PP functional.

Figure 6 depicts a plot of $C(t)$ and an exponential fitting function $C_s(t)$. It is seen that the short decay is indeed an exponential (τ for BP and PP are 0.0105 and 0.0145 picoseconds, respectively). If $\langle N \rangle$ equals 0.5 we obtain $k_f = 47.6$ for BP and 34.5 for PP. Apparently, the dynamical properties here are very sensitive to the barrier, and hence to the level of theory used. This situation is quite different from the case of equilibrium structure/thermodynamic properties, where the proton population estimates with BP and PP are quite alike.

The vibrational spectra (like the one shown in Tables 9−11) include only harmonic values. We can easily calculate the velocity correlation functions which can be Fourier transformed to obtain the vibrational spectra another way.[16] These spectra include already anharmonicity and temperature effects. Figure 7 shows the Fourier transform of the proton−proton velocity auto-correlation function. We observe a very similar spectrum for BP and PP although the harmonic values were quite different − 656 and 768 cm^{-1}, respectively, for BP and PP. The MD spectrum is a very broad one, ranging from 400 to 1800 cm^{-1}, which is similar to the situation of $H_5O_2^+$.[16] It indicates that the finite temperature proton vibrational motion is rather similar in these three cases.

The full spectrum for $H_3O_2^-$ is shown in Figure 8. The O−H stretch modes of 3700 cm^{-1} agree well with the harmonic estimates, for example, BP gives two harmonic frequencies,

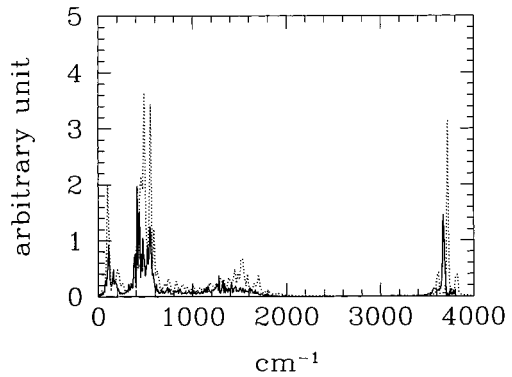

Figure 8. Plot of the vibrational spectra calculated by the BOMD simulation. The solid and dotted lines are results of PP and BP86 functionals, respectively.

3726 and 3728, while PP gives 3698 and 3719 cm^{-1}, respectively. We indeed see higher stretching frequencies for BP in Figure 8. The bending motion at 1500 cm^{-1} is also clearly observed.

Conclusions

The formation of hydrogen bonds in systems involving negatively charged particles are often accompanied by large polarization effects, charge transfer and formation of strong hydrogen bonds. Describing these effects accurately is quite a challenge for contemporary theoretical methods. We should point out that the present study is perhaps the first validation of such a wide range of functionals and methods on hydrated hydroxide anions. It is true that contemporary DFT methods have successfully reached high precision for many systems of chemical interest, but many more remain either out of the DFT scope, or unexplored, and functional success cannot yet be presumed automatically, without concrete validation work. Particularly, the LAP XC functionals, alreadyly validated as of good accuracy for many neutral systems, including hydrogen-bonded ones, appear now to be reliable also for hydrated hydroxide anions, giving precise solvation enthalpies and energetics. The other methods employed in this study also give quite reasonable energetics of the hydrogen bonding in hydroxide anions (within a difference of about 2−15% from the experimental estimate), provided that special care is taken to ensure a high quality basis set and to correct for the bsse. The LAP XC schemes yield slightly improved enthalpies of association of one and two water ligands, compared to the GGA, B3LYP and MP2 results, but comparisons with literature B3LYP and MP2 data is sometimes obscured when the latter studies do not report the bsse correction. The GGA functionals meet some difficulties for the complex with one water, tending to overestimate the binding somewhat, while their performance improves with increasing number of water ligands. Note especially to note the BP functional performance in the case of $n = 3$. The GGA functionals give very low proton-transfer barrier(virtually barrierless), the PLAP value is 0.47 kcal/mol.

The methods are not that comparable in reproducing the geometric structure of the hydroxide complexes, yielding somewhat different hydrogen-bond symmetry and distances, and even a different shape of the complex with three water ligands. These differences are reflected also in the calculated harmonic vibrational spectra at 0 K, particularly concerning the vibrations involving the hydrogen bonds. The latter are expected to exhibit strong anharmonicity, and we have performed also an MD simulation of the vibrational spectra with full account of anharmonicity and finite temperature effects. To our knowledge this is the first attempt of calculating the vibrational spectra of these systems at that level of precision.

The flatness of the potential energy surface associated with the hydrogen bond degrees of freedom leads to an intriguing but complicated proton dynamics in these systems. At 0 K, the optimized structures for BP and PP seem to be quite different. However, their MD population at 300 K is very similar. At 0 K, the geometry optimization searches for the global minimum that might be not much lower in energy than other conformations. The BOMD simulation is able to explore the energy landscape and gives a rather similar free energy profile for the two GGA functionals used. This is also clearly reflected in the similarity of their finite temperature vibrational spectra due to the proton motion. In this sense the situation is quite similar to the case of $H_5O_2^+$. Our conclusion here is quite different from that of Parrinello et al.,[22] where a different XC functional was used and consequently, very different free energy profiles were observed for $H_3O_2^-$ and $H_5O_2^+$. This shows that the choice of the functional does matter in contemporary MD-DFT studies of this kind. Moreover, the proton transfer dynamics is particularly sensitive to the XC functional used, and the results for the proton-transfer counting functions obtained at BP and PP DFT levels are here quite different. It would be interesting to study the proton-transfer dynamics using the LAP functionals, which is the subject of future work. Calculating clusters larger than in the present study will also be in order, which will allow the solvent effect to be examined more fully.

References and Notes

(1) Guo, H.; Sirois, S.; Proynov E. I.; Salahub, D. R. Density Functional Theory and its Application to Hydrogen Bonded Systems. In *Theoretical Treatment of Hydrogen Bonding*; Hadzi, Dusan, Ed.; John Wiley & Sons: New York, 1997. Guo H.; Salahub D. R. *Angew. Chem. Int. Ed.* **1998**, *37*, 2985.

(2) Barone, V.; Adamo, C. *Int. J. Quantum Chem.* **1976**, *61*, 429.

(3) Barone, V.; Adamo, C. *J. Chem. Phys.* **1996**, *105*, 11007.

(4) Becke, A. D. *Phys. Rev. A* **1988**, *38*, 3098.

(5) Perdew, J. P.; Wang, Y. *Phys. Rev.* **1986**, *B33*, 8800. Perdew J. P. *Electronic Structure of Solids*; Ziesche, P., Eschrig, H., Eds.; Academic Verlag: Berlin, 1991.

(6) Lee, C.; Yang, W.; Parr, R. G. *Phys. Rev.* **1988**, *B37*, 785.

(7) Sim F.; St- Amant A.; Papai I.; Salahub D. R. *J. Am. Chem. Soc.* **1992**, *114*, 4391.

(8) Sirois S.; Proynov E. I.; Nguyen D. T.; Salahub D. R. *J. Chem. Phys.* **1997**, *107*, 6770.

(9) Becke A. D. *J. Chem. Phys.* **1993**, *98*, 1372.

(10) Becke A. D. *J. Chem. Phys.* **1993**, *98*, 5648.

(11) Del Bene J. E.; Person W. B.; Szczepaniak, K. *Phys. Chem.* **1995**, *99*, 10705.

(12) Proynov E. I.; Sirois S.; Salahub D. R. *Int. J. Quantum Chem.* **1997**, *64*, 427.

(13) Proynov E. I.; Vela, A.; Ruiz, E.; Salahub, D. R. *Int. J. Quantum Chem. Symp.* **1995**, *29*, 61.

(14) Salahub D. R.; Chretien S.; Milet A.; Proynov, E. I. *Performance of Density Functionals for Transition States* in *Transition State Modeling for Catalysis*; Truhlar, D. G., Morokuma, K., Eds.; ACS Symposium Series 721, American Chemical Society: Washington, DC, 1999.

(15) González, L.; Mó, O.; Yáñez, M. *J. Comput. Chem.* **1997**, *18*, 1124.

(16) Salahub, D. R.; Martinez, A.; Wei, D. Q. In *Theory of Atomic and Molecular Clusters*; Jellinek, J., Ed.; Springer: New York, 1998.

(17) Schenewerk, M. S.; Palmer, P.; Sydner, L. E.; De Pater, I. *Astron. J.* **1986**, *92*, 166.

(18) Beveridge, A. J.; Heywood, G. C. *Biochemistry* **1993**, *32*, 3325.

(19) Pan, Y.; McAllister, M. A. *J. Am. Chem. Soc.* **1997**, *119*, 7561.

(20) Pudzianowski, A. T. *J. Chem. Phys.* **1996**, *100*, 4781.

(21) Pudzianowski A. T. *J. Chem. Phys.* **1995**, *102*, 8029.

(22) Tuckerman, M. E.; Marx, D.; Klein, M. L.; Parrinello, M. *Science* **1997**, *275*, 817.

(23) Meot-Ner (Mautner) M.; Speller, C. V. *J. Phys. Chem.* **1986**, *90*, 6616.

(24) Payzant, J. D.; Yamdagni, R.; Kebarle, P. *Can. J. Chem.* **1971**, *49*, 3308.

(25) Ashadi, M.; Kebarle, P. *J. Phys. Chem.* **1970**, *74*, 1483.

(26) De Paz, M.; Giardini, A. G.; Friedman, L. *J. Chem. Phys.* **1970**, *52*, 687.
(27) Szczesniak, M. D.; Scheiner, S. J. *J. Chem. Phys.* **1982**, *77*, 4586.
(28) McMichael Rohlfing, M.; Allen, L. C.; Cook, C. M. *J. Chem. Phys.* **1983**, *78*, 2498.
(29) Sapse, A. M.; Osorio, L.; Snyder, G. *Int. J. Quantum Chem.* **1984**, *26*, 223.
(30) Newton, M. D.; Ehrenson, S. *J. Am. Chem. Soc.* **1971**, *93*, 4971.
(31) Ohta, K.; Morokuma, K. *J. Phys. Chem.* **1985**, *89*, 5845.
(32) Xantheas, S. S. *J. Am. Chem. Soc.* **1995**, *117*, 10373.
(33) Grimm, A. R.; Bacskay, G. B.; Haymet, A. D. J. *Mol. Phys.* **1995**, *86*, 369.
(34) Dunning, T. H., Jr. *J. Chem. Phys.* **1989**, *90*, 1007. Kendall, A.; Dunning, T. H., Jr.; Harrison, R. J. *J. Chem. Phys.* **1992**, 96, 6769.
(35) Del Bene, J. E. *J. Phys. Chem.* **1988**, *92*, 2874.
(36) St- Amant, A.; Salahub, D. R. *Chem. Phys. Lett.* **1990**, *169*, 387.
(37) Casida, M. E.; Daul, C. D.; Goursot, A.; Koester, A.; Pettersson, L.; Proynov, E. I.; St-Amant, A.; Salahub, D. R. principal authors; Duarte, H.; Godbout, N.; Guan, J.; Jamorski, C.; Lebouf, M.; Malkin, V.; Malkina, O.; Sim, F.; Vela, A. (contributing authors) *deMon Software−deMon-KS3 Module*; Université de Montréal: Montreal, 1996.
(38) Hehre, W. J.; Ditchfield, R.; Pople, J. A. *J. Chem. Phys.* **1972**, *56*, 2257. Clark, T.; Chandrasekhar, J.; Schleyer, P. V. R. *J. Comput. Chem.* **1983**, *4*, 294. Krishnan, R.; Binkley, J. S.; Seeger, R.; Pople, J. A. *J. Chem. Phys.* **1980**, *72*, 650.
(39) Sadlej, A. J. *Collect. Czech. Chem. Commun.* **1988**, *53*, 1995.
(40) Godbout, N.; Salahub, D. R.; Andzelm, J.; Wimmer, E. *Can. J. Chem.* **1992**, *70*, 560.
(41) Frisch, M. J.; Trucks, G. W.; Schlegel, H. B.; Gill, P. M. W.; Johnson, B. G.; Robb, M. A.; Cheeseman, J. R.; Keith, T.; Petersson, G. A.; Montgomery, J. A.; Raghavachari, K.; Al-Laham, M. A.; Zakrzewski, V. G.; Ortiz, J. V.; Foresman, J. B.; Peng, C. Y.; Ayala, P. Y.; Chen, W.; Wong, M. W.; Andres, J. L.; Replogle, E. S.; Gomperts, R.; Martin, R. L.; Fox, D. J.; Binkley, J. S.; Defrees, D. J.; Baker, J.; Stewart, J. P.; Head-Gordon, M.; Gonzalez, C.; Pople, J. A. *Gaussian 94*, Revision B.2; Gaussian, Inc.: Pittsburgh, PA, 1995.
(42) Schlegel, H. B. *Ab Initio Methods in Quantum Chemistry−I*; John Wiley & Sons: New York, 1987.
(43) Boys, S. F.; Bernardi, F. *Mol. Phys.* **1970**, *19*, 553.
(44) Hehre, W. J.; Radom, L.; Schleyer, P. V. R.; Pople, J. A. *Ab Initio Molecular Orbital Theory*; John Wiley & Son: New York, 1985.
(45) Vosko, S. H.; Wilk, L.; Nusair, M. *Can. J. Phys.* **1980**, *58*, 1200.
(46) Verlet, L. *Phys. Rev.* **1967**, *159*, 98.
(47) Smith, P. E.; Pettitt, B. M.; Karplus, M. *J. Phys. Chem.* **1993**, *97*, 6907.
(48) Agmon, N. *J. Chim. Phys.* **1996**, *93*, 1714.
(49) Tschumper, G. S.; Schaefer, H. F., III *J. Chem. Phys.* **1997**, *107*, 2529.
(50) Owrutsky, J. C.; Rosenbaum, N. H.; Tack, L. M.; Saykally, R. J. *J. Chem. Phys.* **1985**, *83*, 5338; **1986**, *84*, 5308. Smith, J. R.; Kim, J. B.; Lineberger, W. C. *Phys. Rev.* **1997**, *55*, 2036.
(51) Harris, D. C.; Bertolucci, M. D. *Symmetry And Spectroscopy*; Dover: New York, 1989.
(52) Ojamäe, L.; Shavitt, I.; Singer, S. J. *Int. J. Quantum Chem.* **1995**, *29*, 657.
(53) Perrin, C. L.; Nielson, J. B. *Annu. Rev. Phys. Chem.* **1997**, *48*, 511.